Using bespoke fluorescence microscopy to study the soft condensed matter of living cells at the single molecule level

2011 J. Phys.: Conf. Ser. 286 012001

(http://iopscience.iop.org/1742-6596/286/1/012001)

Using bespoke fluorescence microscopy to study the soft condensed matter of living cells at the single molecule level

Q Xue, O Harriman and M C Leake[1]
Clarendon Laboratory, Dept of Physics, Parks Road, Oxford University, Oxford OX1 3PU, UK

E-mail: m.leake1@physics.ox.ac.uk

Abstract. The use of bespoke imaging tools and analysis can offer significant insight into the living counterpart of soft condensed matter. The soft matter of biological systems consists of molecular building blocks, a staple of which is protein. Protein molecules, so small that 1 billion would fit on the full-stop at the end of this sentence, carry out most of the vital activities in living cells. Many of these processes require the assembly of multiple proteins into remarkable biological machines. Obtaining the blueprints for the architecture of these machines is essential for understanding the workings of the cell. Here, we discuss recent biological physics experiments on functional single-celled organisms in which one can apply bespoke fluorescence microscopy imaging and analysis to monitor the number and dynamics of several different proteins at the nanometre length scale to a precision of single molecules.

1. Introduction

One of the greatest discoveries in the life sciences, made in the 19th century, was that living organisms were composed of cells, and the make-up of cells is what we could describe as soft condensed matter, stuff like DNA, fats and proteins. Much life science research as we know it today is essentially concerned with understanding the mesoscopic molecular mechanisms that make this soft-matter perform the functions of life. But why study such molecular details in living cells when one can do so in the test-tube? The test-tube environment is significantly more controllable, less contaminated and comes with less measurement noise. The best answer is that cells are not test-tubes. A test-tube experiment is a much reduced version of the native biology with only the components which one thinks/hopes are important included. But we now know definitively that even the simplest cells are not just bags of chemicals, but rather have localized processes in both space and time. A related issue is that of localized effects of the physical and chemical environment in the cell which are essentially impossible to faithfully replicate in the test-tube. Also, the effective numbers of molecules involved in many processes are often low, sometimes just a few per cell, and these minimal stoichiometry conditions are not easy to reproduce in the test-tube.

A second question is why use fluorescence microscopy as a measuring tool. In many cases, some of which we illustrate here, it allows us to visualize specific molecular machines inside living cells with relatively minimal perturbation to the native physiology, so in other words it is a relatively gentle probe which allows one to see molecular detail of soft-matter without disrupting it. Here, we will show how the limits of fluorescence microscopy can be pushed towards a single-molecule

[1] To whom any correspondence should be addressed.

precision over an imaging time scale which is realistic in light of the underlying process being studied, in other words in "real time", exploring a sampling rate from Hz up to kHz; a range of three orders of magnitude for characteristic time scale which encapsulates many vital biological processes [1, 2].

2. Counting single molecule subunits in molecular machines using bespoke TIRF

It is relatively easy to see single fluorescent molecules in vitro using bespoke laser excitation total internal reflection fluorescence, or so-called TIRF (figure 1), illustrated here with green fluorescent protein (GFP) molecules binding transiently to a glass coverslip. If we draw a region of interest around each of these spots of light and sum the pixel intensity, this gives us a measure for total photon emission flux. We can observe firstly the total emission flux is relatively constant across a population of molecules, secondly each molecule photobleaches in a step-like manner, the size of the step being a function not only of local laser excitation intensity but also of the immediate physical and chemical environment. This has significance if the molecule is inside a living cell; the absolute brightness depends not only on where in that cell it is but also on what the cell happens to be doing at that time.

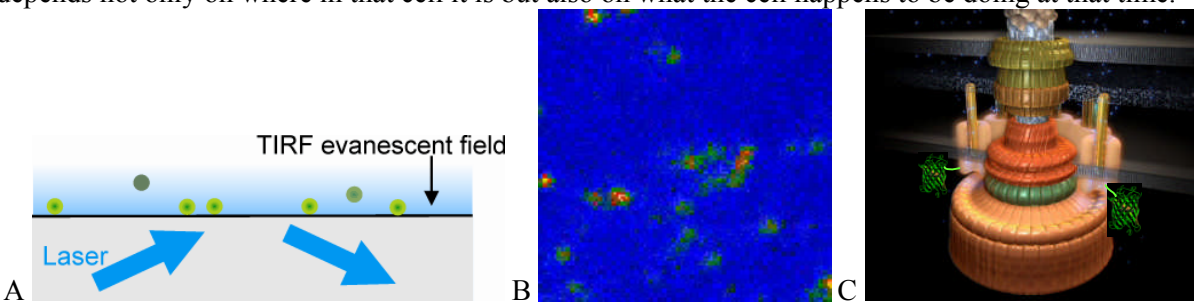

Figure 1. (A) Schematic of transient binding of GFP to a glass coverslip in a TIRF excitation field. (B) Typical experimental single frame snapshot of single GFP molecules bound to glass (false-colour). (C) Schematic of the bacterial flagellar motor molecular machine with attached GFP tags (green).

One example of live-cell imaging involves whole cell motility in bacteria. Bacteria swim by the concerted rotation of several semi stiff helical filaments rotating as one super-filament, at the base of which is an intricate and remarkable molecular machine known as the bacterial flagellar motor (figure 1), one of Nature's primordial wheels. By tinkering with the genetics of the cell so as to fuse GFP to one of the proteins implicated in force generation in this machine, so-called MotB, every molecule of MotB produced will then have a GFP fused to it as a single-molecule fluorescent tag [3]. To visualize this motor one can use a cell rotation assay in which the cell is tethered to a microscope coverslip via one of its filaments. Since the motor is still functional this then causes the whole body of the cell to rotate about this point, like holding down a car wheel and watching the whole car rotate. In TIRF, sampling at typically 1-10 Hz, one generally sees a spot of light at the centre of cell rotation.

One can then quantify fluorescence in exactly the same way as was done with the previous in vitro assay by drawing a region of interest around the spot of intensity. One sees typically exponential photobleach decays, though towards the end of the bleach there is step-like behaviour, made clearer on expanded sections (figure 2). It is more complicated than the in vitro example because the contribution of additional background fluorescence not associated with the motor itself needs to be taken into account, but the principle is the same. One can measure the underlying periodicity in the intensity by constructing a pair-wise difference distribution and then look at its associated power spectrum, which here indicates a fundamental peak at around five thousand counts on our detector. By looking more closely at less noisy data from cells in which the background component was pre-bleached one indeed sees steps of roughly integer multiples of this value. In other words this is an assay that can now pull out the brightness of a single GFP molecule which is unique not only to that single cell, but to that individual molecular machine in that single cell. Dividing the extrapolated initial unbleached intensity by this measured GFP brightness gives an estimate for stoichiometry, here of around 22 molecules.

The width on this distribution is ~6 molecules, but simulations and other experiments show that much of this is inherent variation in the cell population.

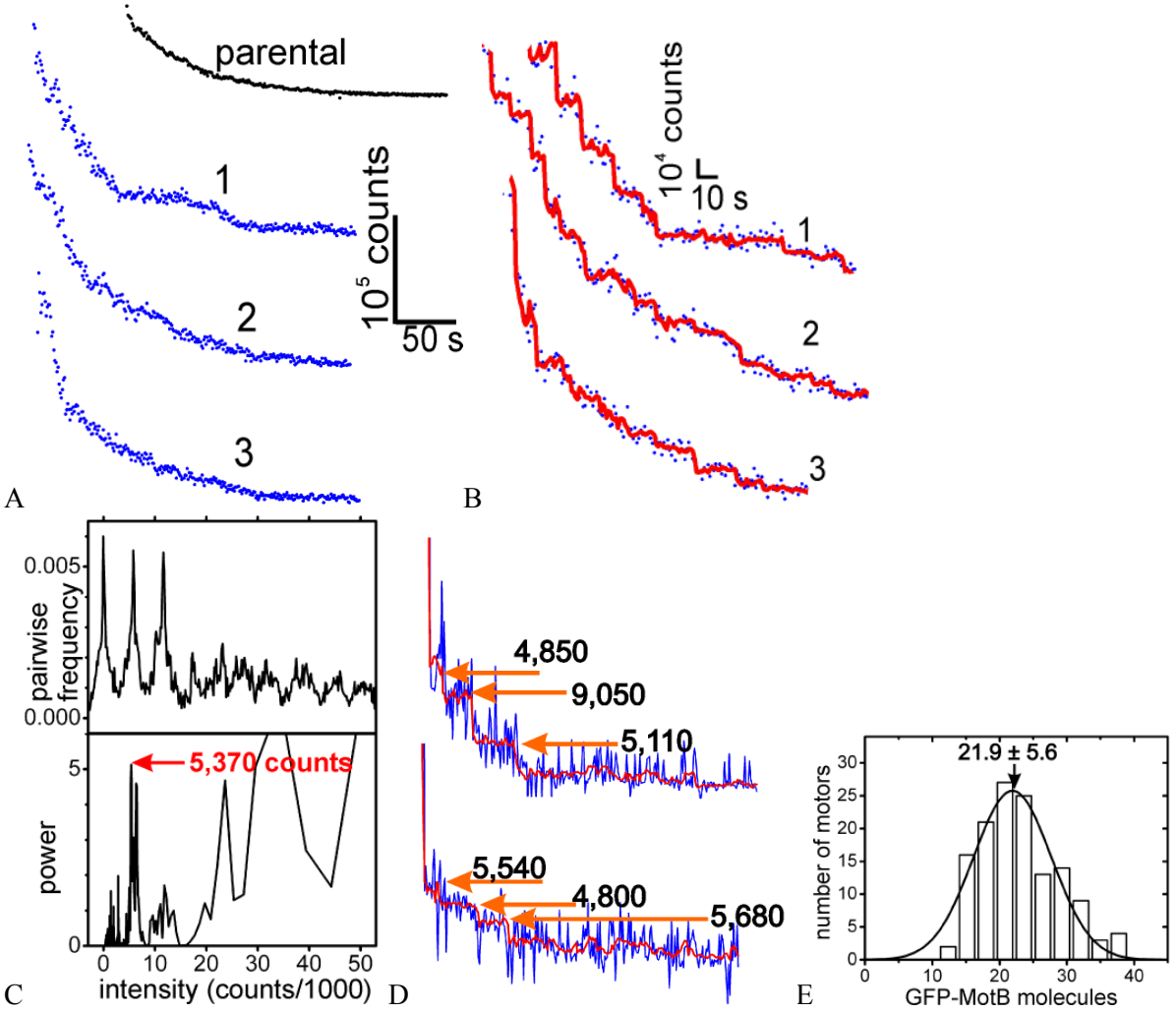

Figure 2. (A) Three typical photobleach intensity traces with (B) expanded sections, raw (blue) and filtered (red) indicated. (C) Pair-wise difference distribution and associated power spectrum. (D) Expanded photobleach sections of pre-bleached cells, step size indicated (arrows). (E) Distribution of molecular stoiochiometry for MotB molecule in the bacterial flagellar motor, Gaussian fit indicated.

2.1. Simulating photobleaching and stoichiometry measurement

To characterize the accuracy of our estimates we generate realistic simulations of the photobleach process using known values for stoichiometry and run these through the same analysis algorithms. We assume that photobleaching is characterized by a series of unitary photobleach events whose probability for occurrence is Poisson distributed. We add in realistic background camera noise in addition to independent photon emission noise from each photoactive fluorescent molecule present in the measurement region of interest (figure 3). This indicates that the overall precision in our stoichiometry estimates using this method is ~10% or less [4].

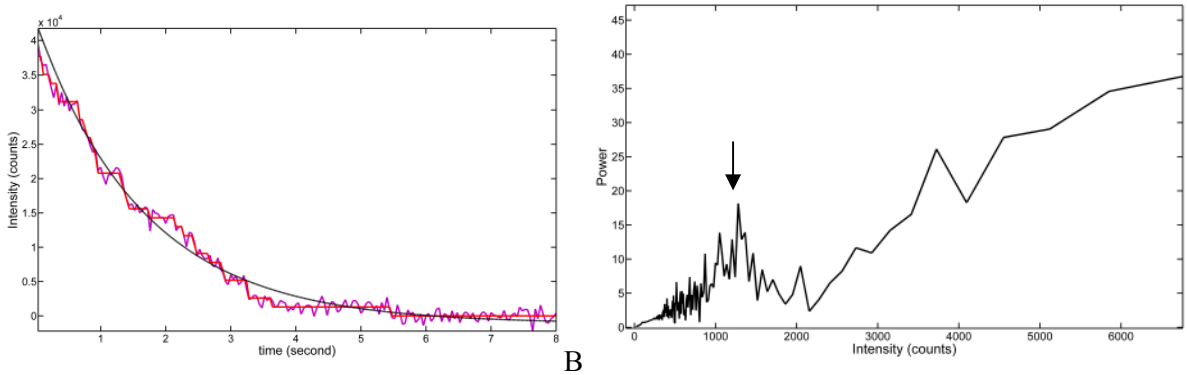

A B

Figure 3. (A) Simulated photobleach, noise-free (red), noise-added (magenta), exponential fit (black) indicated, using 30 initial photoactive proteins, unitary step here of 1,300 counts. (B) Power spectrum of pair-wise difference distribution indicating correct estimation of peak at ~1,300 counts (arrow).

3. Dynamics of single molecules in the cell membrane and turnover in molecular machines

Furthermore, one can monitor protein dynamics. Here one first delimits a high intensity volume using a bespoke focused laser for use in fluorescence recovery after photobeaching, so-called FRAP (figure 4). Looking closely at the cell indicates initially two spots of light, then a flash, then just one spot of light; photobleaching one motor but leaving another motor in the same cell but only one micron away relatively unaffected. There are non-motor components to fluorescence which include a membrane component not incorporated in the motor, and one can monitor the recovery of this component after the focussed laser bleach, showing there must be membrane proteins free to diffuse back into the bleached region, which we can model using Monte Carlo simulations utilising the known geometry of the cell and imposing different values of theoretical diffusion coefficient, and by comparing these to the experimental data we can estimate an effective diffusion coefficient (figure 4). A complementary approach is to track spots of intensity directly as they diffuse on a faster time scale, and both approaches broadly agree to give an estimate which is similar to those of other free membrane proteins of similar mass, so in other words when MotB is not incorporated into a motor it is relatively mobile.

For a motor inside the bleach zone half of the intensity recovers after a period of five minutes. Similarly, for a motor outside the bleach zone its intensity falls by a similar amount over the same time. This is fluorescence loss in photobleaching (FLIP), and what this means is that turnover of the MotB protein has occurred, either involving photobleached or photoactive GFP depending upon its position relative to the centre of the focused laser bleach. Modelling this using a modified Monte Carlo with a diffusion-to-capture element, indicates that the dwell time for a force-generating unit in the motor is ~30 seconds. This is rapid, like driving a car down a motorway but changing one of the wheels at the same time. One unresolved question is whether this turnover is unique to the flagellar motor or is a more generic feature of many different molecular machines.

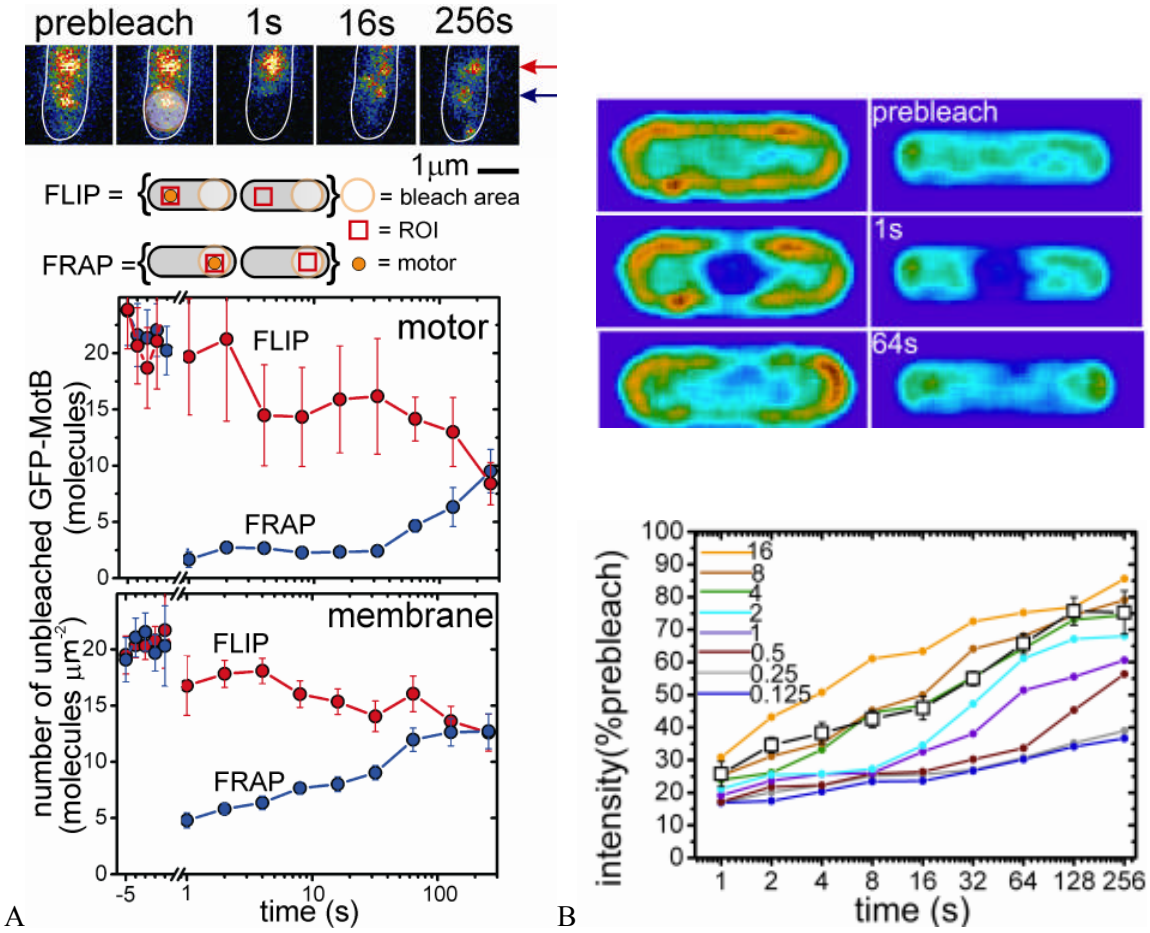

Figure 4. (A) FRAP/FLIP to measure molecular turnover, bleach zone (circle) centred over one motor in a bacterial cell (blue arrow), with another motor in same cell outside the bleach zone (red arrow), changes to intensity of different components indicated. (B) Monte Carlo simulations of bleaching and diffusion in a single cell (upper panel), intensity recovery of membrane component indicated for simulations as a function of time post bleach, effective diffusion coefficients indicated in units of $\mu m^2 s^{-1}$ (coloured lines), compared against experimental values (black squares).

3.1. Tracking molecular machines

To apply similar stoichiometry assays to diffusing membrane proteins requires robust methods for tracking them. To do so one can first automatically segment the outlines of cells, and use this to both generate image masks and cell vital statistics which can be used in coordinate transformations to map between the camera and the curved surface of each cell [5, 6]. Particles can be automatically detected in each fluorescence image and tracked, typically sampling at 10-100 Hz, using an iterative Gaussian fitting process [7]. One can beat the optical resolution limit of roughly half a wavelength by increasing the number of photons sampled, and this is the basis for Fluorescence Imaging at the one nanometre level (FIONA). Having robust tracking implies pulling out the right numbers, and here simulation is everything. One can generate realistic point spread functions using either full 3D Bessel formulations or the experimentally measured point spread function directly, adding noise at realistic levels. A bacterial cell membrane is not a 2D plane, so one can add in a more realistic curved geometry, modelling the cell surface as a cylinder capped by hemispheres, and set simulated particles to diffuse on that surface, figure 5 shows four such particles which start in a row at the bottom of the cell, and two focal planes have been simulated, one through the midline which might be used during epifluorescence, and one at the bottom which might be used in TIRF. These data are run through the

same automated detection and tracking algorithms to predict how well they perform, and the conclusion is that under video-rate conditions the sensitivity is equivalent to around 1 or 2 fluorescent protein molecules with an associated localization precision of 30-40 nm. If a typical diffusing complex has a stoichiometry of the order of 10s of molecules then this localization precision drops to 5 nm or less, the width of a cell membrane.

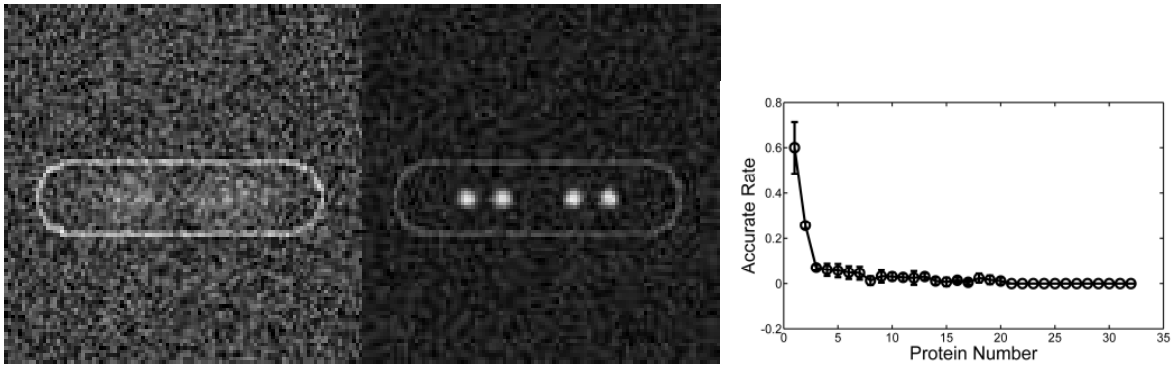

Figure 5. Simulating realistic images of molecular machine diffusion of over cell membranes, showing epifluorescence (left panel), TIRF (middle panel) and the localization precision ("accurate rate") in units of pixels as a function of number of fluorescent proteins per molecular machine.

4. Visualizing molecular machines inside the cell using fast bespoke "slimfield" imaging

The live-cell examples discussed thus far involved membrane proteins at relatively low concentration. There are advantages to this, one is that molecular machines can be imaged using TIRF since they are relatively close to the coverslip surface, second that since they are at low concentration the mean separation is generally greater than the point spread function width and so distinct complexes can be detected. Even in systems having higher concentrations bespoke optical tricks can be applied to effectively reduce the number of photoactive proteins present, either using stochastic photoactivation or photobleaching of a sub-population [8, 9]. A third advantage is that complexes diffuse relatively slowly, so are easier to track. Using simple diffusion theory one can calculate that mobile membrane proteins need to be imaged faster than around 100 ms to be seen unblurred, whereas the limit for proteins inside the cell, in the cytoplasm, is more like just a few milliseconds, typically 3 or less. This means that conventional video-rate imaging is too slow, and simply reducing the image time per frame results in the signal being swamped by noise. The test cytoplasmic system we studied was that of DNA replication, again using a model bacterial organism. DNA replication is performed by a multiprotein machine in the cytoplasm called the replisome. Previously, several functional cell strains were made which had all 10 or so of the different components of this machine individually labelled with a fluorescent tag, this time with a yellow fluorescent protein called YPet, typical epifluorescence snapshots showing either one or two spots per cell depending upon the stage in the cell growth cycle.

To probe this machine with a better "real time" precision, we used a simple optical trick to generate bespoke "slimfield" illumination [10]. This essentially involves underfilling the back aperture of an objective lens to produce a laterally expanded confocal volume wider than a diffraction-limited focal waist, which can be catered to be large enough to encompass single bacterial cells with relatively little correction needed for non-uniformity in intensity. The effect is to produce a high intensity in the vicinity of single cells allowing ~kHz sampling rates whilst still being above the camera noise. By doing this we could see distinct spots frame by frame on the millisecond time scale (figure 6) and were able to generate step-like photobleach traces to a single-molecule precision [11].

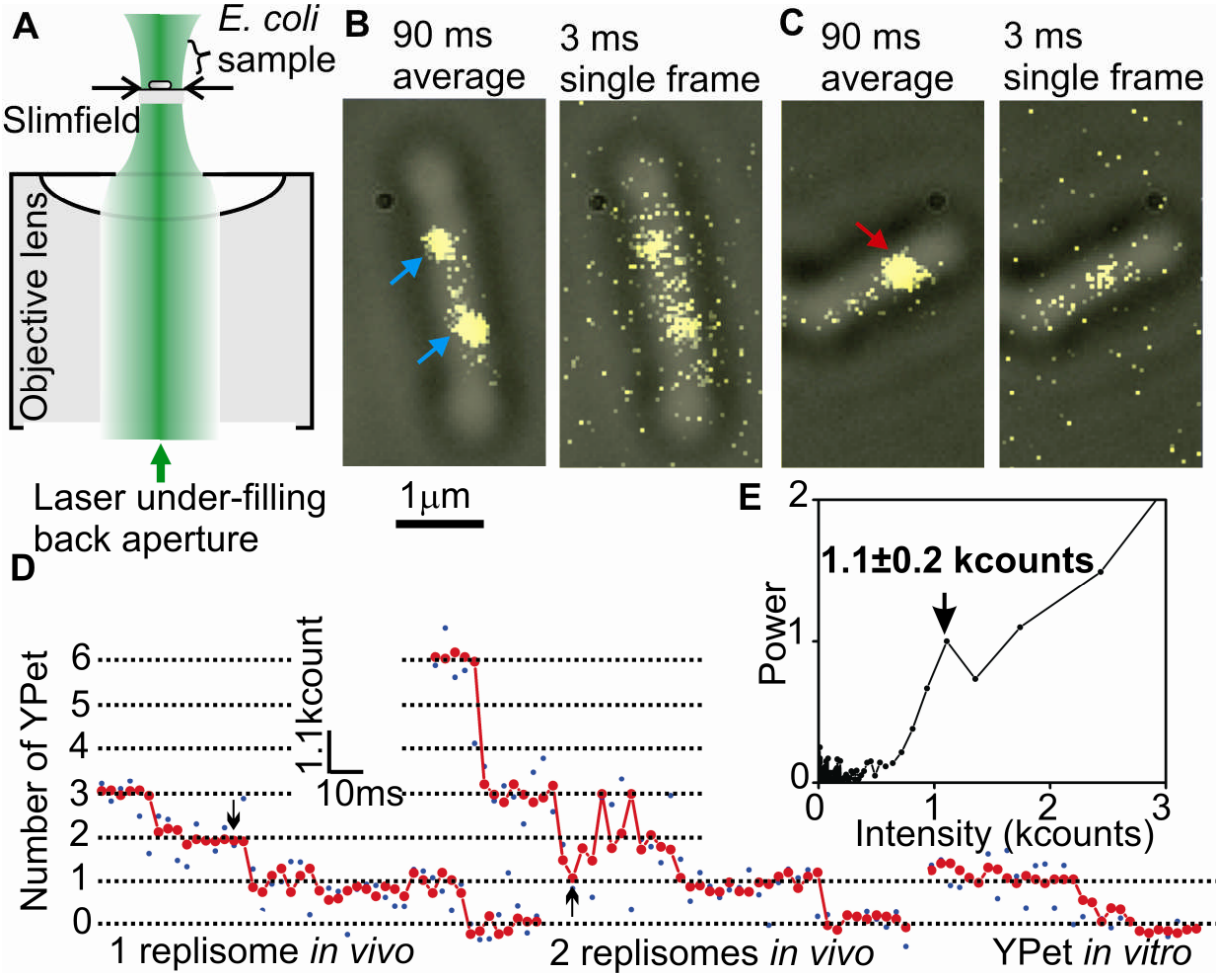

Figure 6. (A) Schematic of slimfield illumination. Images of bacterial cells for which a component of the DNA polymerase enzyme DnaQ has been fused to YPet, either having (B) 2 spots or (C) 1 spot per cell. (D) Typical photobleach trace from spots in cells which had two spots per cell (left panel) and in cells which had one spot per cell (right panel) compared against a single photobleach step for purified surface immobilized YPet in vitro, and (E) power spectrum of pair-wise difference distribution for photobleach trace showing unitary peak brightness.

5. Conclusions

Here we show how using a combination of bespoke optical microscopy and image analysis the unitary photobleach step of fluorescent proteins can be measured in a variety of living cells, in order to apply this as a measuring tool for estimating the stoichiometry of components within functional molecular machines. Furthermore, one can extend the bespoke microscopy and imaging to permit tracking of mobile machines in the cell membrane, and can push the sampling limit up the kHz level to permit imaging of biological machines in the cytoplasm of living cells. The immediate future development of this work lies in extending these methodologies into the multi-colour regime (figure 7), which should allow measurement of two or more different protein components in the same cell at the same time, which may go some way to addressing several questions of living soft condensed matter complexity.

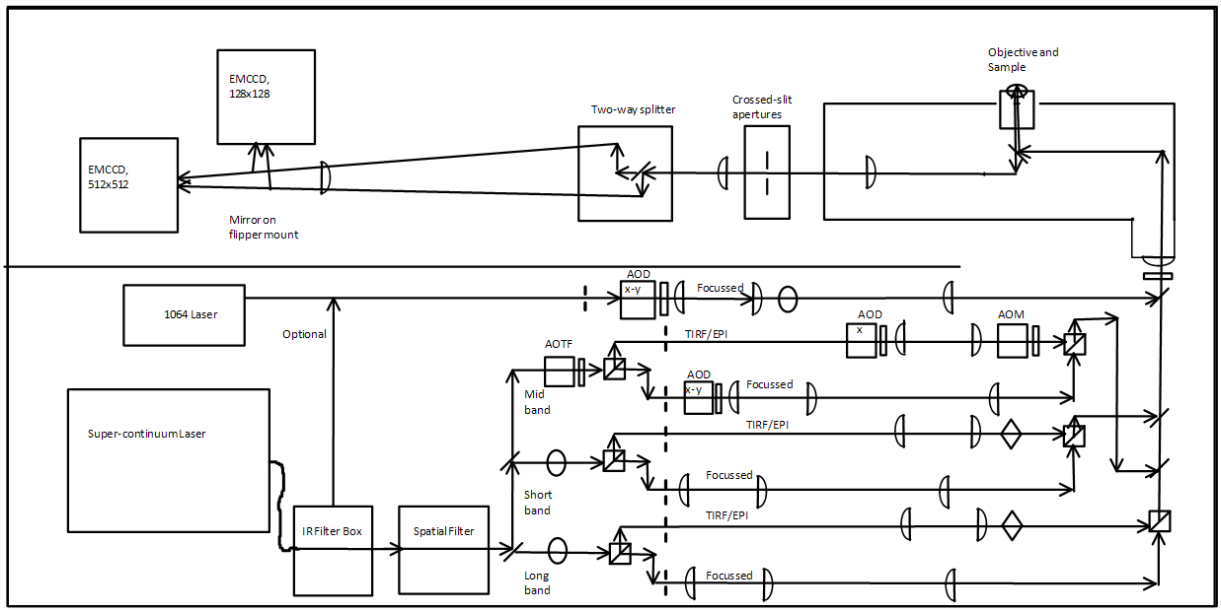

Figure 7. Optical path diagram for a new bespoke microscope setup permitting multi-colour imaging over "real time" scales spanning several orders of magnitude (work in progress, O. Harriman).

6. References

[1] Leake MC 2010 *Commun Integr Biol.* **3** 415
[2] Dobbie IM, Robson A, Delalez N and Leake MC 2009 *J Vis Exp.* **31** 1508
[3] Leake MC, Chandler JH, Wadhams GH, Bai F, Berry RM and Armitage JP 2006 *Nature* **443** 355
[4] Delalez NJ, Wadhams GH, Rosser G, Xue Q, Brown MT, Dobbie IM, Berry RM, Leake MC, and Armitage JP 2010. *Proc Natl Acad Sci U S A* **107** 11347
[5] Leake MC, Greene NP, Godun RM, Granjon T, Buchanan G, Chen S, Berry RM, Palmer T and Berks BC 2008 *Proc Natl Acad Sci U S A* **105** 15376
[6] Xue Q, Jones NS and Leake MC 2010 *Proc. IEEE Internat. Symp. Biomed. Imaging (ISBI): From Nano to Macro* 161
[7] Xue Q and Leake MC 2009 *Proc. IEEE Internat. Symp. Biomed. Imaging (ISBI): From Nano to Macro* 1158
[8] Lenn T, Leake MC and Mullineaux CW 2008 *Mol Microbiol.* **70** 1397
[9] Lenn T, Leake MC and Mullineaux CW 2008 *Biochem Soc Trans.* **36** 1032
[10] Plank M, Wadhams GH and Leake MC 2009 *Integr Biol (Camb)* **10** 602
[11] Reyes-Lamothe R, Sherratt DJ and Leake MC 2010 *Science* **328** 498

Acknowledgments

This research was supported by a Royal Society University Research Fellowship (M.C.L.), BBSRC via the Oxford Centre for Integrative Systems Biology (Q.X.), EPSRC (O.H. and M.C.L.), the Oxford University Press (M.C.L) and a Hertford College Oxford Research Fellowship (M.C.L.)